

High-pressure durable flexible tactile actuator based on microstructured dielectric elastomer

Dongbum Pyo,^{1,2} Semin Ryu,¹ Ki-Uk Kyung,¹ Sungryul Yun,² and Dong-Soo Kwon^{1,a)}

¹Korea Advanced Institute of Science and Technology (KAIST), 291 Daehak-ro, Yuseong-gu, Daejeon 34143, South Korea

²Electronics and Telecommunications Research Institute (ETRI), 218 Gajeong-ro, Yuseong-gu, Daejeon 34129, South Korea

(Received 18 November 2017; accepted 20 January 2018; published online 6 February 2018)

We demonstrate a robust flexible tactile actuator that is capable of working under high external pressures. The tactile actuator is based on a pyramidal microstructured dielectric elastomer layer inducing variation in both mechanical and dielectric properties. The vibrational performance of the actuator can be modulated by changing the geometric parameter of the microstructures. We evaluated the performance of the actuator under high-pressure loads up to 25 kPa, which is over the typical range of pressure applied when humans touch or manipulate objects. Due to the benefit of nonlinearity of the pyramidal structure, the actuator could maintain high mechanical output under various external pressures in the frequency range of 100–200 Hz, which is the most sensitive to vibration acceleration for human finger pads. The responses are not only fast, reversible, and highly durable under consecutive cyclic operations, but also large enough to impart perceivable vibrations for haptic feedback on practical wearable device applications. © 2018 Author(s). All article content, except where otherwise noted, is licensed under a Creative Commons Attribution (CC BY) license (<http://creativecommons.org/licenses/by/4.0/>). <https://doi.org/10.1063/1.5016385>

Flexible and wearable electronic devices have received much attention as promising candidates to satisfy the demands for revolutionary designs for human-computer interactions. Since tactile interfaces have been considered as essential components for contemporary electronic devices, technologies to implement tactile sensing and feedback functionality on flexible geometries have been widely studied. To provide tactile feedback with mechanical robustness against geometric changes, electro-active polymers (EAPs), particularly dielectric elastomers (DEs), have been used for soft actuators due to their reversibly large strains with a fast response, cost effectiveness, light weight, and simple manufacturing process.^{1–3} There have been many attempts to amplify the actuation strain of dielectric elastomers^{1,4} and to transform the in-plane strain into large vertical deformation with a passive layer^{5,6} or a stacking structure of multi-layered DE membranes.^{7–9} Although these approaches provide a promising route to human-perceivable tactile response on flexible interfaces, there are still challenges in securing reliable tactile feedback including structural sustainability against pressurized contact and in designing a resonance frequency to be in the human-sensitive frequency range due to the difficulty in modulating intrinsic mechanical properties. As an alternative to resolve these issues, hydrostatically coupled dielectric elastomer actuators (DEAs) using an intermediate fluid between the active membrane and passive part^{10,11} and bistable electroactive polymer (BSEP) actuators modulating their stiffness through Joule heating^{12,13} have been recently proposed. The former facilitates self-compensation of local deformation resulting from a pressurized contact by

improving the initial stiffness of the entire actuator; however, the packaging problem hinders securing durable performance with mechanical robustness and environmental stability. The latter allows a refreshable braille display maintaining a deformed state through stepwise procedures, including thermally induced softening, electrical actuation, and stiffening by air-cooling; however, its operating principle is unsuitable for providing immediate tactile information. For practical application of soft actuators in wearable devices, the actuators need to be improved to produce effective tactile feedback under external loads as high as 20 kPa, which is a typical pressure for user's touch.^{8,14,15}

Here, we propose a flexible tactile actuator with a microstructured DE layer that is capable of producing a robust vibrotactile response under high external pressures for user's contact. As illustrated in Fig. 1(a), the tactile actuator is composed of a flexible DE layer with monolithic pyramidal geometry and two parallel polyethylene terephthalate (PET) films with an indium tin oxide (ITO) electrode. Due to the benefits of the nonlinear structural design, the DE layer allows high mechanical output in the human-sensitive frequency range (100–200 Hz) of perception for acceleration.^{16–19} The actuator is capable of tuning the dynamic performance by modulating the compressive modulus and dielectric property of the DE layer through the change in geometric parameters. The actuation performance for the vibrotactile response is fast (response delay: <2 ms) and durable (performance degradation: <15% for 250 000 cycles). Since the overall vibration acceleration is much higher than the tactile threshold under high external pressures up to 25 kPa, similar to a user's touch environment, the tactile actuator can allow wearable devices to provide reliable tactile stimuli in practical applications.

^{a)}Author to whom correspondence should be addressed: kwonds@kaist.ac.kr. Tel.: +82-42-350-3042. Fax: +82-42-350-8240.

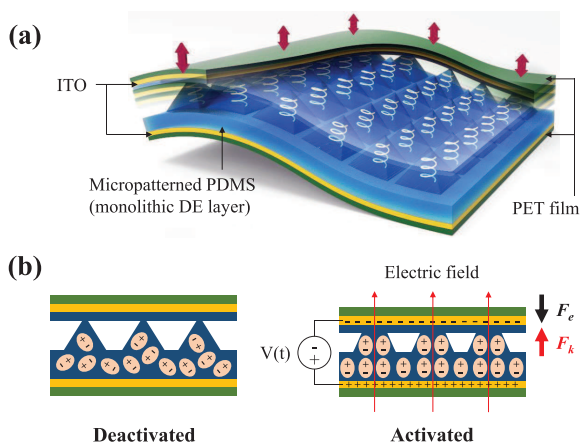


FIG. 1. Schematics of (a) structural configuration and (b) operating principle of microstructured DEA generating vibration in the normal direction due to the interaction between an elastic reaction force (F_k) and an electrostatic attraction force (F_e).

Figure 1(b) shows the operating principle of the pyramidal microstructured DEA. When the biased positive sinusoidal voltage is applied to the ITO electrodes, the electrostatic pressure arising from coulomb forces acts between the electrodes and the electrostatic attraction force compresses the parallel-arranged microstructures; thus, elastic restoring force is stored in the microstructures. When the amplitude of the biased sinusoidal voltage decreases, the microstructures return to their original shape reversibly and generate reaction forces in the thickness direction.

The DEA was fabricated monolithically including the microstructures, and the schematically illustrated fabrication process is shown in Fig. 2. We fabricated an inverted pyramid silicon mold using an anisotropic wet etching technique, which is commonly used for the fabrication of micromechanical structures. Since the etched angle is 54.74° , the width of

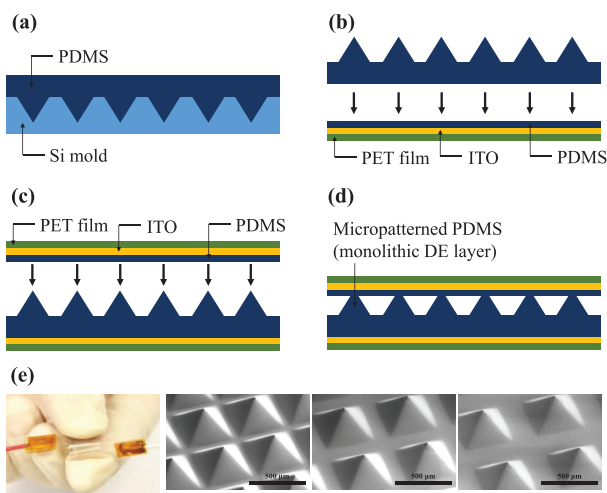


FIG. 2. Schematic illustration of the fabrication process for microstructured DEA: (a) casting PDMS solution on a silicon mold and (b) and (c) spin coating the solution on two ITO electrode-coated PET films and integrating with the microstructured DE layer, respectively. (d) Fabricated monolithic microstructured DEA. (e) Photograph of the flexible microstructured DEA (left) images of the pyramid structures (spatial distances of 500, 600, and 700 μm , in order) obtained using a Magellan400 scanning electron microscope (right). The scale bar is 500 μm .

the pyramid with height h is determined as $2h/\tan(54.74^\circ)$. A polydimethylsiloxane (PDMS) elastomer solution (Elastosil[®] P7670 A/B, Wacker Chemie AG) with a mixture ratio of 1:1 was transferred onto the mold and spin-coated at 200 rpm for 60 s. Thereafter, it was cured at 65°C for 30 min under vacuum. After peeling off the pyramidal microstructured DE layer from the mold, it was integrated with two ITO-coated PET films (surface resistance, $60\ \Omega/\text{sq}$; thickness, 5 mil; Sigma-Aldrich Co.) with a thin elastomer solution coating, which was prepared by spin-coating at 9000 rpm for 20 s (thickness, 5 μm). Finally, the integrated structure was constructed by curing under the same environment. A series of DEAs using pyramidal microstructured DEs with different spatial distances of 500, 600, and 700 μm were prepared by maintaining the pyramid height of 300 μm , substrate thickness of 300 μm , and area of 100 mm^2 . The series of DEAs are henceforth denoted as S_{500} , S_{600} , and S_{700} , respectively. The spatial distance denotes the distance between the centers of the pyramids.

Considering that high-pressure endurance can be strongly correlated with mechanical and dielectric properties, we intensively investigated the changes in both the characteristics with changing geometric parameters. The compressive moduli of different microstructured DEAs and unstructured DEA (thickness, 600 μm) were measured using a dynamic mechanical analyzer (DMA, RSA-G2, TA Instruments). The stiffnesses of the pyramidal microstructured DEAs, which have a highly nonlinear characteristic, are significantly lower than that of the unstructured DEA, as shown in Fig. 3(a). This indicates that the pyramidal microstructured DEA can generate a considerably larger displacement than the unstructured DEA due to the high compressibility. With the increasing spatial distance, that is, with decreasing density of the microstructures, the DEA becomes more compressible.

To evaluate the dielectric characteristics of the different pyramidal microstructured DEAs, the effective dielectric constant was measured under the same environment and numerical simulation was performed under an electric field of 5 MV/m using commercially available simulation software, as shown in Fig. 3(b). With the decreasing spatial distance, the electrostatic attraction force increased in the order $S_{700} < S_{600} < S_{500}$ because of the increase in the effective dielectric constant between the electrodes. As the pyramidal microstructured DEA is compressed, the electrostatic attraction force increases nonlinearly due to the decreasing gap distance and the increasing effective dielectric constant between the parallel electrodes. However, the nonlinear increase in the electrostatic force does not cause geometry of the microstructure to collapse from electromechanical pull-in instability because it is always lower than the elastic reaction force when a microstructured DE layer is compressed by external pressure.^{20–22}

Figure 4 shows the effect of different mechanical and dielectric behaviors of the DEAs on the dynamic response. The displacement amplitude in the vertical direction was measured by placing loads (50 g and 200 g) on the DEA using a scanning vibrometer (Polytec PSV-500) with a sampling rate of 25 kHz. The resonance frequency increased with increasing stiffness of the DEA. Consequently, changing the spatial distance from 700 μm to 500 μm caused the

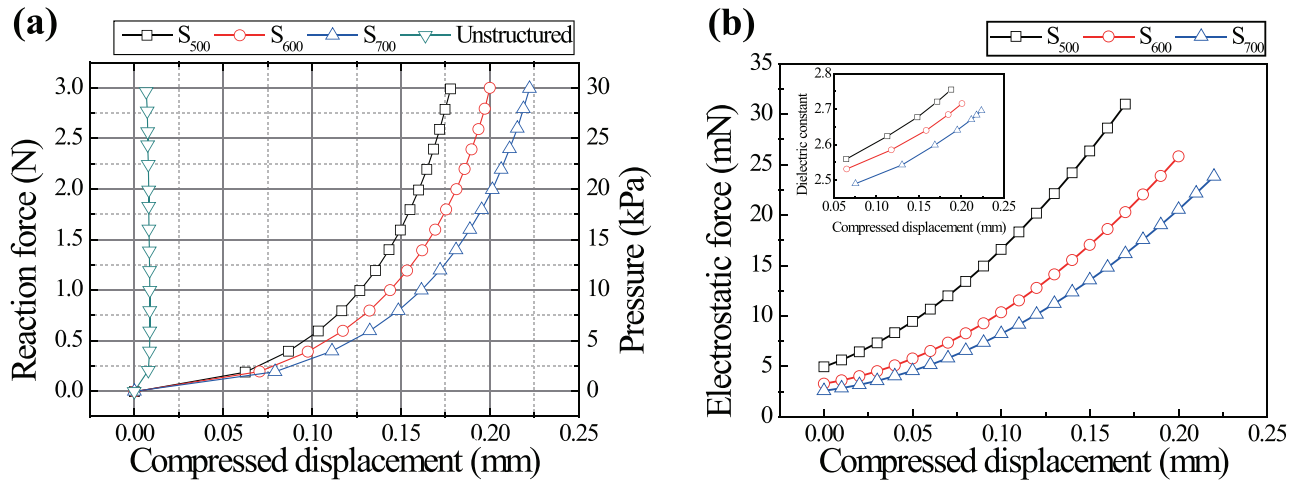


FIG. 3. Variations in mechanical and dielectric characteristics of pyramidal microstructured DEAs as a function of compressed displacement in accordance with geometric parameters: (a) elastic reaction force; (b) electrostatic attraction force, and effective dielectric constant (inset).

shifting of resonance frequency from 95 and 90 Hz to 115 and 105 Hz at external pressures of 5 and 20 kPa, respectively. This implies that the resonance of the DEA can be designed by modulating the compressive modulus, especially in the frequency range of 100–200 Hz, where humans are sensitive to vibration acceleration.

Although S_{500} is disadvantageous in generating vertical displacement because it is less compressible than others are, it produced the largest peak displacement amplitude because of the higher electrostatic attraction forces applied under the same electric field, which compensate for this, resulting in larger displacement. The reduction in the dielectric property (effective dielectric constant) due to the increase in compressibility affects the generation of vertical displacement. The results indicate that the improved performance of the microstructured DEA should result from the balance between compressibility and dielectric characteristics.

Figure 5(a) presents the frequency characteristics of S_{500} for vertical displacement under various external pressures. Compared to the previously reported unstructured thickness-mode DEA (vertical deformation in the frequency range of 100–200 Hz, about $6 \mu\text{m}$; resonance frequency, 1500 Hz;

electric field, 15 MV/m),⁶ the microstructured DEA produced a larger vertical displacement of over $10 \mu\text{m}$ at a resonance frequency of 160 Hz under a low electrical field of 5 MV/m and an external pressure of 1 kPa. In addition, as the external load increased, the resonance frequency varied in the frequency range of 100–200 Hz due to the highly nonlinear elastic characteristics of the pyramidal microstructured DE layer. The resonance frequency of the system, which had a linear elastic spring, decreased as the mass of the system increases, but that of the pyramidal microstructured DEA increases again from the point at which the rate of increase in stiffness was greater than the rate of increase in mass. Therefore, the DEA could maintain high mechanical output in the desired frequency range.

We note that microstructuring of the DE layer has advantages not only in designing the resonance frequency of the DEA but also in generating perceivable vibration acceleration even at an external pressure as high as 25 kPa, which is significantly higher than the previously evaluated vibrotactile threshold (AL: Absolute limen)^{18,19} in the frequency range of 100–200 Hz, as shown in Fig. 5(b). This implies that the proposed DEA in wearable devices can produce sufficient tactile feedback from users' touch in daily activities.

The displacement responses with respect to the sinusoidal input signals are reversible, as shown in Fig. 5(c). Even at an external pressure of 20 kPa, the responses follow the input signals with a fast response time of 2 ms, which is enough for immediate transmission of tactile feedback.²³ In addition, the displacement stabilizes after a small decrease of 14% during 250 000 consecutive cyclic operations under an external pressure of 20 kPa (decrease of 9% at 5 kPa), as shown in Fig. 5(d). The performance degradation is also observed in typical DE membrane actuators that produce electrically induced deformation.²⁴ However, because the small decrease in displacement is lower than previously reported just-noticeable-differences (JNDs) of 1.5–2.5 dB (18.9–33.3%) for the intensity of tactile stimulus, the actuator can provide reliable haptic feedback to the user.^{25,26}

In conclusion, we have developed a flexible tactile actuator with a pyramidal microstructured elastomer allowing robust operation under user's touch in daily activities for

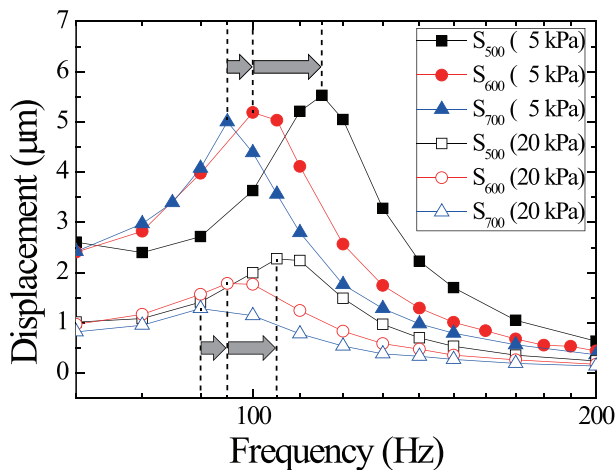


FIG. 4. Effect of different mechanical and dielectric behaviors of DEAs on the dynamic response.

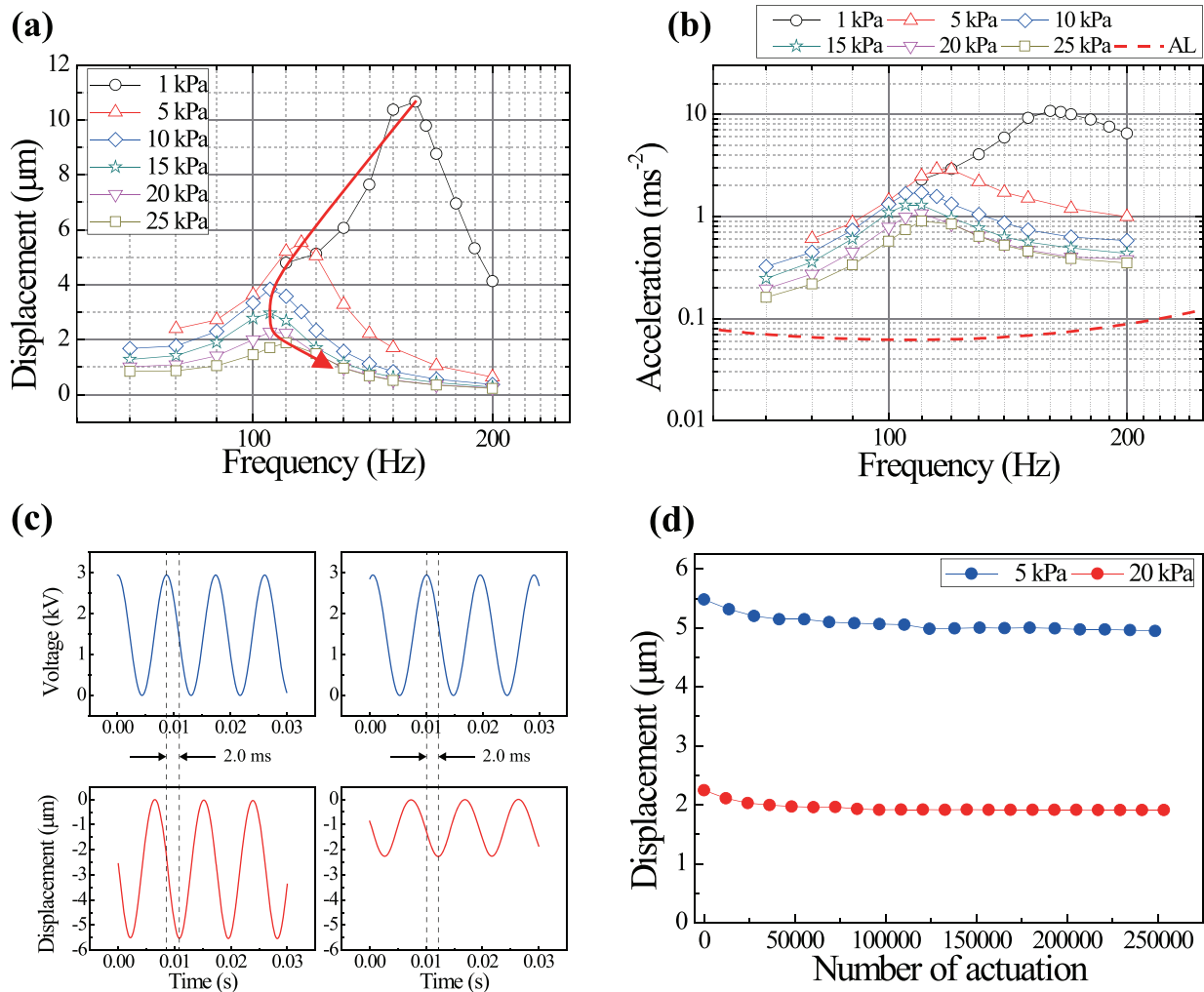


FIG. 5. Performance of microstructured DEA (S_{500}). Frequency characteristics for (a) vertical displacement and (b) vibration acceleration with vibrotactile threshold curve (AL: Absolute limen). (c) Sinusoidal input voltage-displacement profile with time at 115 Hz (resonance) under 5 kPa (left) and 105 Hz (resonance) under 20 kPa (right). (d) Displacement profile during consecutive cyclic operations at 115 Hz (resonance) under 5 kPa and 105 Hz (resonance) under 20 kPa.

wearable devices. Microstructuring of the DE layer enables the generation of large displacement and acceleration in the vertical direction under external pressure as high as 25 kPa, thus achieving high-pressure sustainability and to allow designing resonance frequency. Due to the benefit of non-linearity of the pyramid structure, the tactile actuator could maintain high mechanical output in the frequency range of 100–200 Hz, which is sensitive to vibration acceleration for human fingertips. The tactile actuator produces fast, reversible, and durable responses under continuous cyclic operations responding to sinusoidal input-voltage signals. Experimental evaluations of vibrational performance with changing geometric parameters of the microstructures revealed that the mechanical and dielectric properties of the microstructured DEA should be balanced to improve the performance. The microstructured DEA with high-pressure endurance has the potential for practical wearable device applications.

This work was supported by the Pioneer Program of Korea National Research Foundation (No. 2013M3C1A3059557) and the Electronics and Telecommunications Research Institute

(ETRI) grant funded by the Korean government (No. 18ZS1300, the development of smart context-awareness foundation technique for major industry acceleration).

- ¹R. Pelrine, R. Kornbluh, Q. Pei, and J. Joseph, *Science* **287**(5454), 836 (2000).
- ²Q. M. Zhang, V. Bharti, and X. Zhao, *Science* **280**(5372), 2101 (1998).
- ³R. Shankar, T. K. Ghosh, and R. J. Spontak, *Adv. Mater.* **19**(17), 2218 (2007).
- ⁴G. Kofod, M. Paaajanen, and S. Bauer, *Appl. Phys. A* **85**(2), 141 (2006).
- ⁵H. Prahlad, R. Pelrine, R. Kornbluh, P. von Guggenberg, S. Chhokar, J. Eckerle, M. Rosenthal, and N. Bonwit, in *Electroactive Polymer Actuators and Devices (EAPAD)* (2005), pp. 102–114.
- ⁶S. Yun, S. Park, B. Park, S. K. Park, H. Prahlad, P. Von Guggenberg, and K. U. Kyung, *IEEE/ASME Trans. Mechatronics* **19**(4), 1463 (2014).
- ⁷I. M. Koo, K. Jung, J. C. Koo, J. D. Nam, Y. K. Lee, and H. R. Choi, *IEEE Trans. Rob.* **24**(3), 549 (2008).
- ⁸M. Matysek, P. Lotz, T. Winterstein, and H. F. Schlaak, in *World Haptics Conference 2009 (WHC 2009)* (IEEE, 2009), pp. 290–295.
- ⁹P. Lotz, M. Matysek, and H. F. Schlaak, *IEEE/ASME Trans. Mechatronics* **16**(1), 58 (2011).
- ¹⁰F. Carpi, G. Frediani, and D. De Rossi, *IEEE/ASME Trans. Mechatronics* **15**(2), 308 (2010).
- ¹¹H. S. Lee, H. Phung, D.-H. Lee, U. K. Kim, C. T. Nguyen, H. Moon, J. C. Koo, J.-D. Nam, and H. R. Choi, *Sens. Actuators, A* **205**, 191 (2014).

- ¹²Z. Yu, W. Yuan, P. Brochu, B. Chen, Z. Liu, Q. Pei, T. Mirfakhrai, J. D. W. Madden, and R. H. Baughman, *Appl. Phys. Lett.* **95**(19), 192904 (2009).
- ¹³X. Niu, X. Yang, P. Brochu, H. Stoyanov, S. Yun, Z. Yu, and Q. Pei, *Adv. Mater.* **24**(48), 6513 (2012).
- ¹⁴D. G. Caldwell, N. Tsagarakis, and C. Giesler, in *Robotics and Automation* (IEEE, 1999), pp. 287–292.
- ¹⁵Y. Zang, F. Zhang, C. an Di, and D. Zhu, *Mater. Horiz.* **2**(2), 140 (2015).
- ¹⁶K. O. Johnson, *Curr. Opin. Neurobiol.* **11**(4), 455 (2001).
- ¹⁷L. Kruger, M. P. Friedman, and E. C. Carterette, *Pain and Touch* (Academic Press San Diego, 1996).
- ¹⁸H.-U. Ko, H. C. Kim, J. Kim, and S.-Y. Kim, *Smart Mater. Struct.* **24**(5), 055018 (2015).
- ¹⁹M. Morioka and M. J. Griffin, *Somatosens. Mot. Res.* **22**(4), 281 (2015).
- ²⁰R. Pelrine, R. Kornbluh, and J. Joseph, *Sens. Actuators, A* **64**(1), 77 (1998).
- ²¹J. Plante and S. Dubowsky, *Int. J. Solids Struct.* **43**(25), 7727 (2006).
- ²²D. Tommasi, G. Puglisi, G. Saccomandi, and G. Zurlo, *J. Phys. D: Appl. Phys.* **43**(32), 325501 (2010).
- ²³I. Poupyrev, S. Maruyama, and J. Rekimoto, in *User Interface Software and Technology (UIST)* (ACM, 2002), pp. 51–60.
- ²⁴S. Yun, S. Park, B. Park, S. Nam, S. Park, and K. Kyung, *Appl. Phys. Lett.* **107**(8), 081907 (2015).
- ²⁵J. Craig, *Percept. Psychophys.* **11**(2), 150 (1972).
- ²⁶A. Israr and H. Tan, *J. Acoust. Soc. Am.* **120**(5), 2789 (2006).